Published in final edited form as:
Nano Lett. 2009 February ; 9(2): 914–918. doi:10.1021/nl900096z.

Electrical Recording from Hearts with Flexible Nanowire Device Arrays

Brian P. Timko[1,†], **Tzahi Cohen-Karni**[1,‡], **Guihua Yu**[†], **Quan Qing**[†], **Bozhi Tian**[†], and **Charles M. Lieber**[*,†,‡]

†*Department of Chemistry and Chemical Biology, Harvard University, Cambridge, Massachusetts 02138*

‡*School of Engineering and Applied Science, Harvard University, Cambridge, Massachusetts 02138*

Abstract

We show that nanowire field-effect transistor (NWFET) arrays fabricated on both planar and flexible polymeric substrates can be reproducibly interfaced with spontaneously-beating embryonic chicken hearts in both planar and bent conformations. Simultaneous recordings from glass microelectrode and NWFET devices show that NWFET conductance variations are synchronized with the beating heart. The conductance change associated with beating can be tuned substantially by device sensitivity, although the voltage-calibrated signals, 4–6 mV, are relatively constant and typically larger than signals recorded by microelectrode arrays. Multiplexed recording from NWFET arrays yielded signal propagation times across the myocardium with high spatial resolution. The transparent and flexible NWFET chips also enable simultaneous electrical recording and optical registration of devices to heart surfaces in three-dimensional conformations not possible with planar microdevices. The capability of simultaneous optical imaging and electrical recording also could be used to register devices to a specific region of the myocardium at the cellular level, and more generally, NWFET arrays fabricated on increasingly flexible plastic and/or biopolymer substrates have the potential to become unique tools for electrical recording from other tissue/organ samples or as powerful implants.

Recording electrical signals *in vitro* and *in vivo* from whole hearts represents a general methodology useful in areas ranging from basic studies of cardiac function to patient healthcare.[1–6] Low-resolution measurements of activation across the entire heart with, for example macroscale metallic electrodes in contact with the epicardium[2] or optical microscopy of dyed tissue,[3,4] have been used as a diagnostic tool to examine the origins of arrhythmia.[1–4] More recently, higher-resolution recording from embryonic hearts has been achieved using microelectrode arrays (MEAs) with typical electrode diameters and spacings of order 10 and 100 μm, respectively. MEAs can yield more detailed information than larger scale electrodes, for example, on conduction velocities in heart tissue,[4–6] yet a reduction in signal to noise with decreasing MEA electrode size[7,8] will make microns to submicron resolution measurements needed for cellular or subcellular resolution difficult to achieve. Moreover, higher-resolution MEAs have been restricted to planar structures that cannot conform to organs, such as the heart, which are intrinsically three-dimensional (3D) soft objects.

An alternative method for electrical recording from biological systems uses NW and carbon nanotube FETs as key device elements.[9,10] These nanoscale FETs have demonstrated higher sensitivity than planar devices for recording local potential changes associated with binding and unbinding of proteins, nucleic acids and viruses[11–14] as well as the propagation of action

*Corresponding authors: Email: cml@cmliris.harvard.edu.
[1]These authors contributed equally to this work

potentials from cultured neurons.[15] To date, NW and nanotube devices have not been used for recording from tissue samples or entire organs, although there are several reasons that make such studies attractive. First, the intrinsic small size of NW and nanotube FETs could provide information about propagating electrical signals at a far higher spatial resolution than previously demonstrated. Second, there is considerable emerging work demonstrating that nanostructures and nanostructured substrates have enhanced interactions with artificial membranes, cells, and tissue compared to larger-scale morphologies and planar substrates.[16–19] Third, NW and nanotube device arrays can be readily fabricated on flexible and transparent polymer substrates,[20–22] and thus device chips could be bent to conform to 3D curved surfaces of a heart versus the case of rigid, planar microdevice arrays.

Here we describe electrical recording from whole embyonic chicken hearts using NWFET arrays in both planar and bent conformations. Briefly, 30 nm diameter p-type Si-NWs[23,24] were transferred to oxidized silicon and transparent polymer substrates, interconnects were defined by standard photolithography and then passivated using a combination of Si_3N_4 and SU-8 polymer films. The fabrication approach yields active NWFET channels that protrude above the surface of the underlying chip almost entirely exposed to solution. The two-layer passivation provides robust isolation of the metal interconnects on planar and highly bent chips with minimal capacitive coupling up to 15 kHz measurement frequencies.

In a typical experiment with planar NWFET chip configuration (Figure 1A,B), a freshly isolated heart[25] was placed on top of the active device region of a heated sample chamber. After a brief period of equilibration with medium, hearts beat spontaneously at a typical frequency of 1–3 Hz for ca. 20 min.[26] Initially, the NWFET response to beating hearts was carried out by simultaneously recording signals from a NWFET and from a conventional glass pipette inserted into the heart.[27] Representative data (Fig. 1C) show close temporal correlation between initial sharp peaks recorded by the two distinct measurements, although the pipette peak occurs ca. 100 ms before the NWFET peak in each beat. The consistent time difference is expected since the pipette was inserted into a spatially remote region with respect to the NWFET devices. Examination of individual NW signals reveals an initial fast phase (full-width at half maximum, FWHM = 6.8 ± 0.7 ms) followed by a slower phase (FWHM = 31 ± 9 ms). NWFET signals exhibiting the fast followed by slow phases were recorded in 85% of our >75 independent experiments, and thus demonstrate the reproducibility of our NW-based recording approach. Notably, measurements remain stable for up to 9 minutes of continuous recording, with long-term experiments ultimately limited by the viability of the excised heart (Figure S1A). In addition, the NWFET arrays are very stable with single chips being used for multiple experiments over the course of several weeks (Figure S1B).

Several experiments were carried out to understand the nature of the two recorded peaks and the role of the NWFET recording elements. First, an inhibitor of myosin-II ATPase activity, blebbistatin, was applied during recording to prevent contraction while maintaining the physiological excitability of ion channels.[29,30] Signals recorded before and after addition of blebbistatin[28] showed that the slow transients were eliminated while the initial, fast transients were unaffected (Figure S2). Hence, the fast phase peaks can be associated with transient ion-channel current in the hearts. Second, simultaneous measurements from adjacent ‘devices’ with and without NWs (with 20 μm inter-device spacing) yielded characteristic signals only for electrodes with the NW element. Taken together these results confirm that NWFET is essential for recording and that the much larger contact electrodes do not contribute to the observed signals.

The peaks recorded with our NWFETs (Figure 1C) exhibit excellent signal-to-noise. The observed conductance changes associated with these peaks does, however, depend on the device transconductance. To illustrate this point and provide voltage calibration for the peaks,

data were recorded at a variety of applied water-gate potentials.[23] NWFET results from a beating heart with the water-gate varied from −0.4 to 0.4 V (Figure 1D,E) show a decrease in the magnitude of the fast transient conductance change from ca. 55 to 11 nS, which is correlated with the decrease in device transconductance over this same range of water-gate potentials. Notably, the voltage-calibrated signal determined using the device transconductance (Figure 1E) was essentially constant at 5.1 ± 0.4 mV for this same variation of water gate voltage. These results confirm the stability of the interface between the NWFETs and beating heart, and highlight the necessity of recording explicit device sensitivity to interpret corresponding voltages. To investigate further the sensitivity and potential spatial resolution of the NWFET elements, measurements were also recorded simultaneously from two NWFETs with a center-to-center separation of only 5 μm (Figure S3A). The conductance peaks recorded from NW1 and NW2 (Figure S3B) have a 1.5x difference in amplitude (10.7 vs. 16.2 nS), although the calibrated voltages are the same. These data also demonstrate the potential to record signals without cross-talk at a spatial resolution substantially higher than with MEAs.

NWs and carbon nanotube FETs can be fabricated on flexible plastic substrates,[20–22] and thus open up the possibility of making chips that can be readily deformed to tissue and organs or used for *in vivo* studies, as demonstrated in the case of polymer-based MEAs.[31,32] We have explored this concept by assembling NWFETs on 50 μm-thick flexible and transparent Kapton substrates. An image of a typical device chip (Figure 2A) highlights its flexibility and transparency, as well as the straightforward pin-plug interface to our recording instrumentation. In these experiments, the NWFET devices are located in a central 4.8 × 1.2 mm^2 region of the chip, although we stress that other configurations are readily accessible simply through fabrication with appropriate photolithography masks. Plots of NW conductance (G) vs. applied water gate voltage (V_g) for three devices in the array (inset, Figure 2A) show that devices all turn off (threshold voltages) close to or positive of $V_g = 0$. In the on-state, the maximum device sensitivities, G/V_g, at $V_g = -0.2$ V are 24, 32 and 22 μS/V for NW1, NW2 and NW3, respectively. We believe that these device variations could be reduced in the future, and stress that they in no way limit quantitative recording from whole hearts.

Specifically, simultaneous measurements made with these three NWFETs from an isolated beating heart (Figure 2B) show correlated fast and slow phase peaks similar to those shown in Fig. 1. The fast phase conductance peaks, which exhibited excellent S/N, had recorded magnitudes of 127 ± 4, 146 ± 4 and 114 ± 4 nS for NW1, NW2 and NW3 respectively. These conductance values correspond to calibrated voltages of 5.3 ± 0.2, 4.6 ± 0.1 and 5.3 ± 0.2 mV, and are comparable to those observed from devices fabricated on rigid silicon/silicon oxide substrates (e.g., Figure 1E). The voltage differences likely reflect small variations in NW/heart interface given the relative separation of NW1, NW2 and NW3 (Figure 2C) but do not affect quantitative analysis of timing differences between the NW recording elements.

To determine possible time differences between the signals recorded by the three NW devices we used a standard cross-correlation technique.[33] The three devices, which had a geometric layout represented by Figure 2C, were interfaced with the ventricular region of the heart such that an axis drawn between the atria and apex was oriented along the line defined by NW1/NW3 and NW2 in the array. In the first orientation, the 1.2 ms time delays between signals recorded by NW1/NW3 and NW2 (Figure 2C, left) reveals an activation sequence corresponding to surface propagation from the apex toward the atria. This conclusion is consistent with known activation sequences across the epicardium of hearts from chick embryos.[35] To confirm the robustness of the measurements, we also rotated the heart 180° and observed a consistent inversion of signal delays (Figure 2C, right). These experiments bear out the potential of flexible NWFET arrays to record wavefront propagation on the surfaces of hearts. The present experiments, which had an instrument limited recording resolution of ca. 300 μs,[33] could not resolve timing delays between NW1 and NW3; however,

implementation of higher bandwidth recording should enable the high spatial resolution of NW devices to be used for such studies in the future.

These flexible and transparent NWFET chips also enable simultaneous optical imaging and electronic recording in configurations that are not readily accessible with traditional planar device chips, yet advantageous for producing diverse, functional tissue-device interfaces. A bent device chip with concave surface facing a beating heart immersed in medium (Figure 3A) illustrates this capability. We note that the chip is readily integrated into an upright microscope and allows for both visual inspection, which enables rough orientation of the device array to the heart, and higher-resolution imaging through the transparent substrate while recording from NWFET devices (Figure 3B). Our capacity for simultaneous imaging of tissue and devices enables their registration at the level of the entire organ down to that of individual cells. Notably, recording from a representative NWFET device in this inverted configuration (Figure 3C) demonstrated excellent S/N fast component peaks correlated with the spontaneously-beating heart. The average magnitude of the conductance peaks, 164 ± 7 nS, and calibrated voltage, 4.5 ± 0.2 mV, are similar to that recorded in more traditional ‘planar’ configuration. In addition, similar recording was achieved on beating hearts in which bent chips were oriented with convex NWFET surface wrapped partially around the heart. Taken together, these results demonstrate that our flexible and transparent NW chips can be used to record electronic signals from organs in configurations not achievable by conventional electronics.

We believe that the demonstration of recording from embryonic hearts using flexible and transparent NWFET arrays presents a number of opportunities for the future. As shown above and elsewhere,[36] NW devices can be readily fabricated with sub-10 μm spacing, with active device areas orders of magnitude smaller than state-of-the-art MEAs,[5,6,37,38] and could provide data at sub-cellular resolution. To exploit this spatial resolution for temporal measurements of firing will, however, require the demonstration of frequency bandwidth greater than demonstrated in the present studies. The capability of simultaneous optical imaging and electrical recording also could be used to register devices to a specific region of the myocardium at the cellular level. Last, we believe that NWFET arrays fabricated on increasingly flexible plastic and/or biopolymer substrates can become unique tools for electrical recording from other tissue/organ samples or as powerful implants.

Supplementary Material

Refer to Web version on PubMed Central for supplementary material.

Acknowledgement

We thank K. Kaminitz and R. Milo for helpful discussions. C.M.L acknowledges support of this work by McKnight Foundation Neuroscience and NIH Director’s Pioneer Awards.

References

1. Zipes, DP.; Jalife, J. Cardiac Electrophysiology: From cell to bedside. Philadelphia: W.B. Saunders; 2004.
2. Taccardi B, Punske BB, Macchi E, LacLeod RS, Ershler PR. Am. J. Physiol. Heart Circ. Physiol 2008;294:H1753. [PubMed: 18263708]
3. Efimov IR, Nikolski VP, Salama G. Circ. Res 2004;94:21. [PubMed: 15242982]
4. Dhein, S.; Mohr, FW.; Delmar, M. Practical Methods in Cardiovascular Research. New York: Springer; 2005. p. 424-445.
5. Reppel M, Pillekamp F, Lu ZJ, Halbach M, Brockmeier K, Fleischmann BK, Hescheler J. J. Electrocardiol 2004;37:104. [PubMed: 15534818]

6. Lu Z-J, Pereverzev A, Liu H-L, Weiergräber M, Henry M, Krieger A, Smyth N, Hescheler J, Schneider T. Cell Physiol. Biochem 2004;14:11. [PubMed: 14976402]
7. Prohaska OJ, Olcaytug F, Pfundner P, Dragaun H. IEEE T. Bio-Med Eng 1986;2:223.
8. Banks DJ, Balachandran W, Richards PR, Ewins D. Physiol. Meas 2002;23:437. [PubMed: 12051313]
9. Patolsky F, Timko BP, Zheng G, Lieber CM. MRS Rev 2007;32:142.
10. Gruner G. Anal. Bioanal. Chem 2006;384:322. [PubMed: 16132132]
11. Zheng G, Patolsky F, Cui Y, Wang WU, Lieber CM. Nat. Biotechnol 2005;23:1294. [PubMed: 16170313]
12. Stern E, Klemic JF, Routenberg DA, Wyrembak PN, Turner-Evans DB, Hamilton AD, LaVan DA, Fahmy TM, Reed MA. Nature 2007;445:519. [PubMed: 17268465]
13. Star A, Tu E, Niemann J, Gabriel J-CP, Joiner CS, Valcke C. P. Natl. Acad. Sci. USA 2006;103:921.
14. Patolsky F, Zheng G, Hayden O, Lakedamyali M, Zhuang X, Lieber CM. P. Natl. Acad. Sci. USA 2004;101:14017.
15. Patolsky F, Timko BP, Yu G, Fang Y, Greytak AB, Zheng G, Lieber CM. Science 2006;313:1100. [PubMed: 16931757]
16. Zhou X, Moran-Mirabal JM, Craighead HG, McEuen PL. Nat. Nanotech 2007;2:185.
17. Stevens MM, George JH. Science 2005;310:1135. [PubMed: 16293749]
18. Sniadecki NJ, Desai RA, Ruiz SA, Chen CS. Ann. Biomed. Eng 2006;34:59. [PubMed: 16525764]
19. Gheith MK, Sinani VA, Wicksted JP, Matts RL, Kotov NA. Adv. Mater 2005;17:2663.
20. McAlpine MC, Friedman RS, Jin S, Lin K, Wang WU, Lieber CM. Nano Lett 2003;3:1531.
21. Javey A, Nam S, Friedman RS, Yan H, Lieber CM. Nano Lett 2007;7:773. [PubMed: 17266383]
22. Takenobu T, Takahashi T, Kanbara T, Tsukagoshi K, Aoyagi Y, Iwasa Y. Appl. Phys. Lett 2006;88:033511.
23. Patolsky F, Zheng G, Lieber CM. Nat. Prot 2006;1:1711.
24. The 30 nm diameter p-type Si-NWs were synthesized as described previously,[11,14,15,23] and were transferred to the surface of oxidized silicon (600 nm thick oxide, NOVA Electronic Materials, Ltd.) or 50-μm thick Kapton polymer strips by either shear transfer[21] or random-deposition method[11, 23]. Passivated source and drain electrodes were deposited using a multilayer photoresist structure[11,14,15] consisting of 300 nm LOR3A (Microchem) and 500 nm 1805 (Shipley). After the developing the electrode pattern, the contacts were metallized by thermal evaporation of Ti/Pd/Ti (1/50/10 nm), and then ca. 60 nm Si_3N_4 was deposited by plasma-enhanced chemical vapor deposition. Last, the substrate was coated with ca. 15 μm SU-8 2015 photoresist (Microchem), and windows were opened over the NW device regions by photolithography.
25. White Leghorn chick embryos (Charles River Labs) were maintained in a humidified incubator (Carolina Biological Supply Company) at 37.5°C, and hearts were isolated from embryos at E10 – E15 stage. Isolated hearts were immediately transferred to a heated sample stage for measurements.
26. All studies were carried at 37.5°C using either Extracellular Medium (150 mM NaCl, 2.5 mM $CaCl_2$, 5 mM KCl, 1 mM $MgCl_2$, 10 mM HEPES, pH=7.38, osmolality = 290 mosm) or with Tyrode solution (Sigma-Aldrich Inc.). In the case of planar configurations, the substrate was covered with medium that was routinely exchanged throughout measurement. NWFET signals recorded from a heart disappeared (reappeared) when the heart was allowed float above the device array surface (and then brought back into contact). In the case of bent configurations, the heart was held in a cell culture dish that had been filled with medium, where the dish was placed on top of a heated stage. Measurements were performed by approaching the heart from above with the bent plastic substrate. Hearts typically exhibited spontaneous rhythmic beating for ca. 20 min. A Ag/AgCl wire was used as a reference electrode. The NW FET conductance was measured with AC bias (8–15 kHz, 30 mV peak-to-peak) with the DC bias set to 0 V. The drain current was amplified with a variable gain amplifier (1211 current preamplifier, DL Instruments, Inc.) and filtered using a lock-in amplifier (DSP dual phas e lock-in, Stanford Research Systems) with time constant set to 300 μs. The output data were recorded using a multichannel A/D converter (Digidata 1440A, Molecular Devices) at an acquisition rate of 20–40 kHz interfaced with a PC running pClamp 10.1 electrophysiology software (Molecular Devices). Post-analysis was completed in Igor Pro (Wavemetrics).
27. Glass pipettes were pulled (P-97 Micropipette Puller, Sutter Instrument Company) from capillary tubing. They were backfilled with Intracellular Medium (125 mM K gluconate, 20 mM KCl, 0.5 mM

$CaCl_2$, 2 mM $MgCl_2$, 10 mM HEPES, 5 mM EGTA, 2 mM Na_2-ATP, pH=7.3, osmolality = 290 mosm). Filled pipettes were contacted with Ag/AgCl wire and mounted on a motorized 3-axis micromanipulator (MP-285, Sutter Instrument Company). Pipettes exhibited typical resistances of 6–8 MΩ. Signals were recorded and amplified with a standard patch clamp amplifier (Axopatch 200B, Molecular Devices) in current-clamp mode with I=0.

28. Blebbistatin was used to decouple excitation and contraction as described previously[29,30]. Briefly, a 100 μM aqueous solution was prepared in a dark room with illumination from a dim red-colored light, and ca. 700 μL Blebbistatin solution, enough to submerge the entire heart, was then added to the chip. After ca. 10 min. soaking time, spontaneous beating was reduced to slight twitching or was eliminated completely.
29. Fedorov VV, Lozinsky IT, Sosunov EA, Anyukhovsky EP, Rosen MR, Balke CW, Efimov IR. Heart Rythym 2007;4:619.
30. Farman GP, Tachampa K, Mateja R, Cazorla O, Lacampagne A, de Tombe PP. Pflugers. Arch 2008;455:995. [PubMed: 17994251]
31. Adams C, Mathieson K, Gunning D, Cunningham W, Rahman M, Morrison JD, Prydderch ML. Nucl. Instrum. Meth. A 2005;546:154.
32. Cheung KC, Renaud P, Tanila H, Djupsund K. Biosens. Bioelectron 2007;22:1783. [PubMed: 17027251]
33. Timing delays were calculated using a standard cross-correlation technique.[34] Briefly, each trace in Figure 2B was loaded in its entirety into Matlab (The Mathworks, Inc.) as a single-column matrix. Each matrix (X_i) was normalized by $X_{i,norm} = (X_i - \mathbf{mean}(X_I)) / \mathbf{std}((X_i - \mathbf{mean}(X_i))$, where **mean** and **std** are standard Matlab functions for calculating mean and standard deviation, respectively. Unbiased cross-correlation analysis was performed on pairs of normalized matrices (X_1, X_2) using the built-in **xcorr** function. The cross-correlation function ($X_1 \star X_2$) is a curve with maximum shifted slightly from zero; this shift represents the time-offset between the paired input matrices. The robustness of this technique was tested by examining paired matrices X_1 and X_2, that were either identical or from separate, multiplexed devices that recorded the same signals. We arbitrarily offset X_2 by 400, 20, 10 or 5 points (corresponding to time shifts of 20 ms, 1 ms, 500 μs and 250 μs, respectively) and observed consistent shifts in the output function $X_1 \star X_2$. In the case of NW1 and NW3 in Figure 2B, the latency was less than the 300 μs time constant of the lock-in amplifier and therefore could not be accurately determined.
34. Augustijn CH, Arts T, Prinzen FW, Reneman RS. Pflugers Arch 1991;419:529. [PubMed: 1775376]
35. Rothenberg F, Watanabe M, Eloff B, Rosenbaum D. Dev. Dynam 2005;233:456.
36. Lu W, Lieber CM. Nat. Mater 2007;6:841. [PubMed: 17972939]
37. Giovangrandi L, Gilchrist KH, Whittington RH, Kovacs GTA. Sensor. Actuat. B-Chem 2006;113:545.
38. Rodger DC, Fong AJ, Li W, Ameri H, Ahuja AK, Gutierrez C, Lavrov I, Zhong H, Menon PR, Meng E, Burdick JW, Roy RR, Edgerton VR, Weiland JD, Humayun MS, Tai Y-C. Sensor. Actuat. B-Chem 2008;132:449.

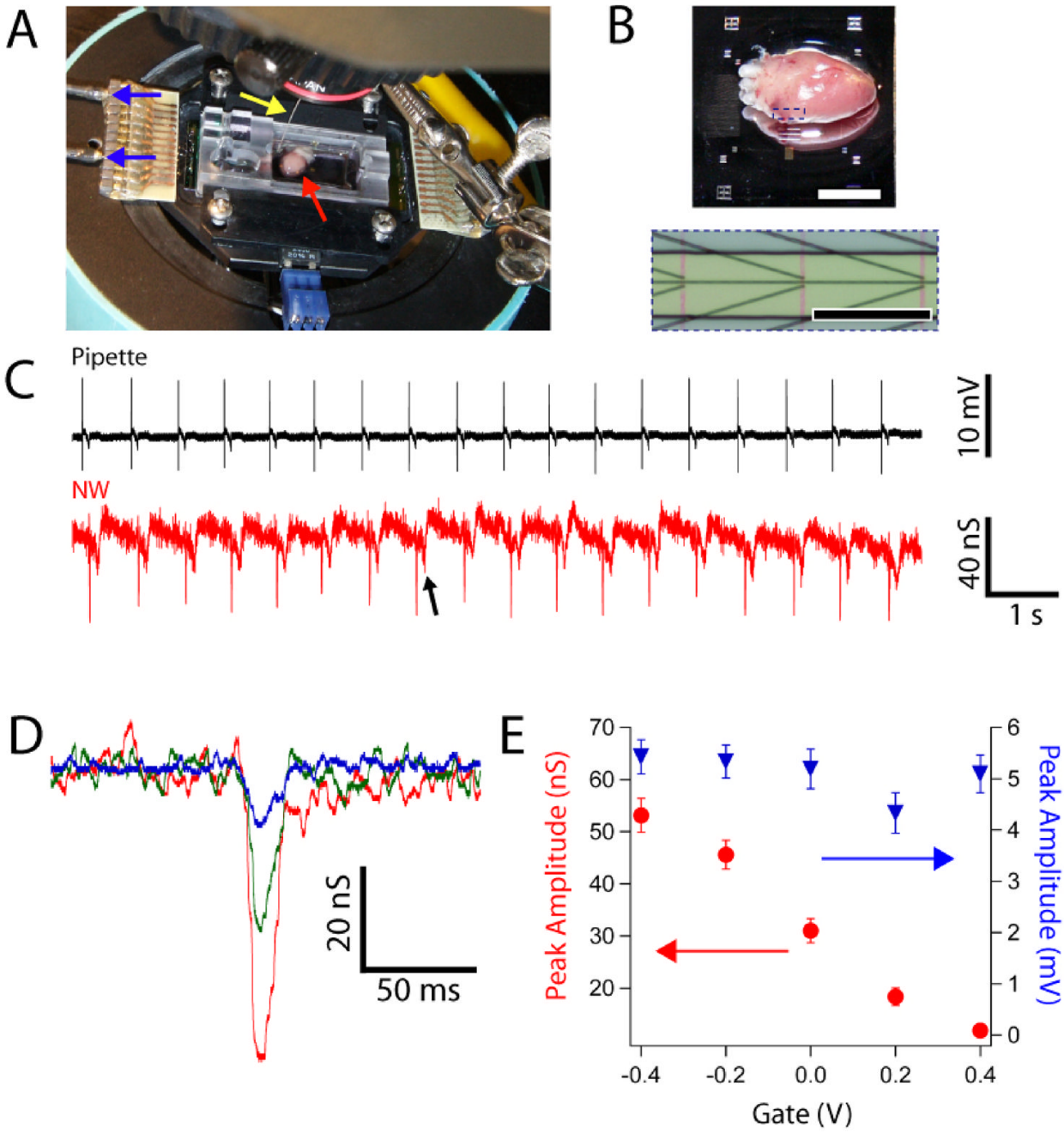

Figure 1. NW/heart interfaces

(A) Photograph of experimental setup showing heart on NWFET chip in temperature regulated cell. Arrows show position of heart (red), Ag/AgCl reference electrode (yellow) and source/drain interconnect wires (blue). (B) (top) Magnified image of heart on surface of planar chip; scale bar is 4 mm. (bottom) Zoom of dotted region in upper image showing three pairs of NW devices; the vertical red lines denote orientation of NWs. Scale bar is 150 μm. (C) Simultaneous recordings from a glass pipette (black trace) and a NW device (red trace). (D) Expansion of single fast transients measured from a heart for $V_g = -0.3$ (red), 0 (green) and 0.3 V (blue). (E) Plots of peak conductance amplitude (red) and calibrated peak voltage amplitude (blue) vs. V_g for same experiment shown in D.

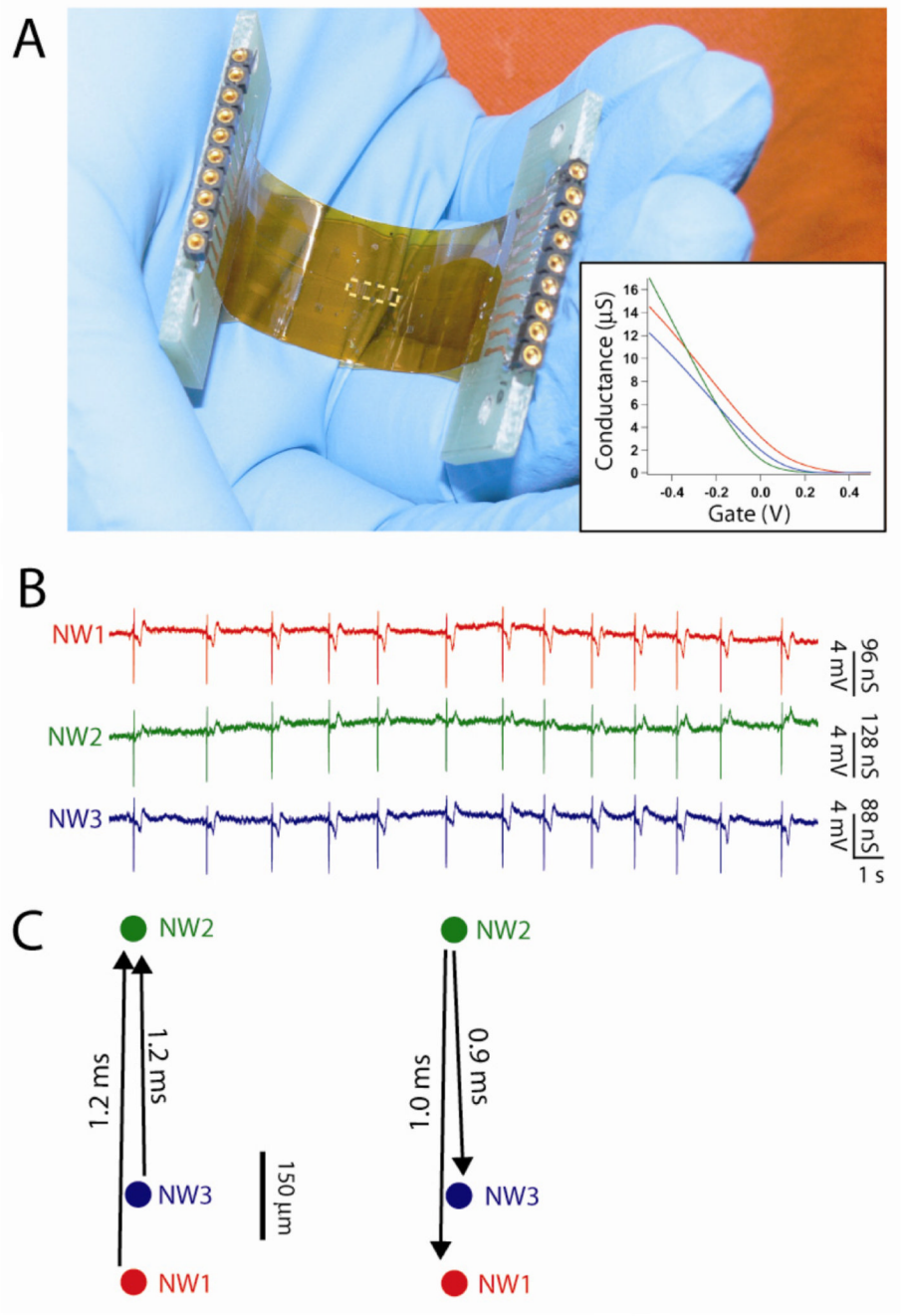

Figure 2. Multiplexed NWFET recording on flexible substrates

(A) Photograph of complete NWFET chip fabricated on a flexible Kapton substrate. The dashed white rectangle at the center of the chip highlights the location of NWFET array. (inset) Conductance vs. water-gate measurements for three representative NWFET devices. (B) Multiplexed device measurements recorded at $V_g = -0.2V$. Conductance measurements were calibrated using the corresponding water-gate data shown in A. (C) (left) Timing shifts[33] between the traces shown in panel B. Arrows indicate latencies between signal recordings from adjacent devices. (right) After rotating heart 180°, latencies are recorded in the opposite direction.

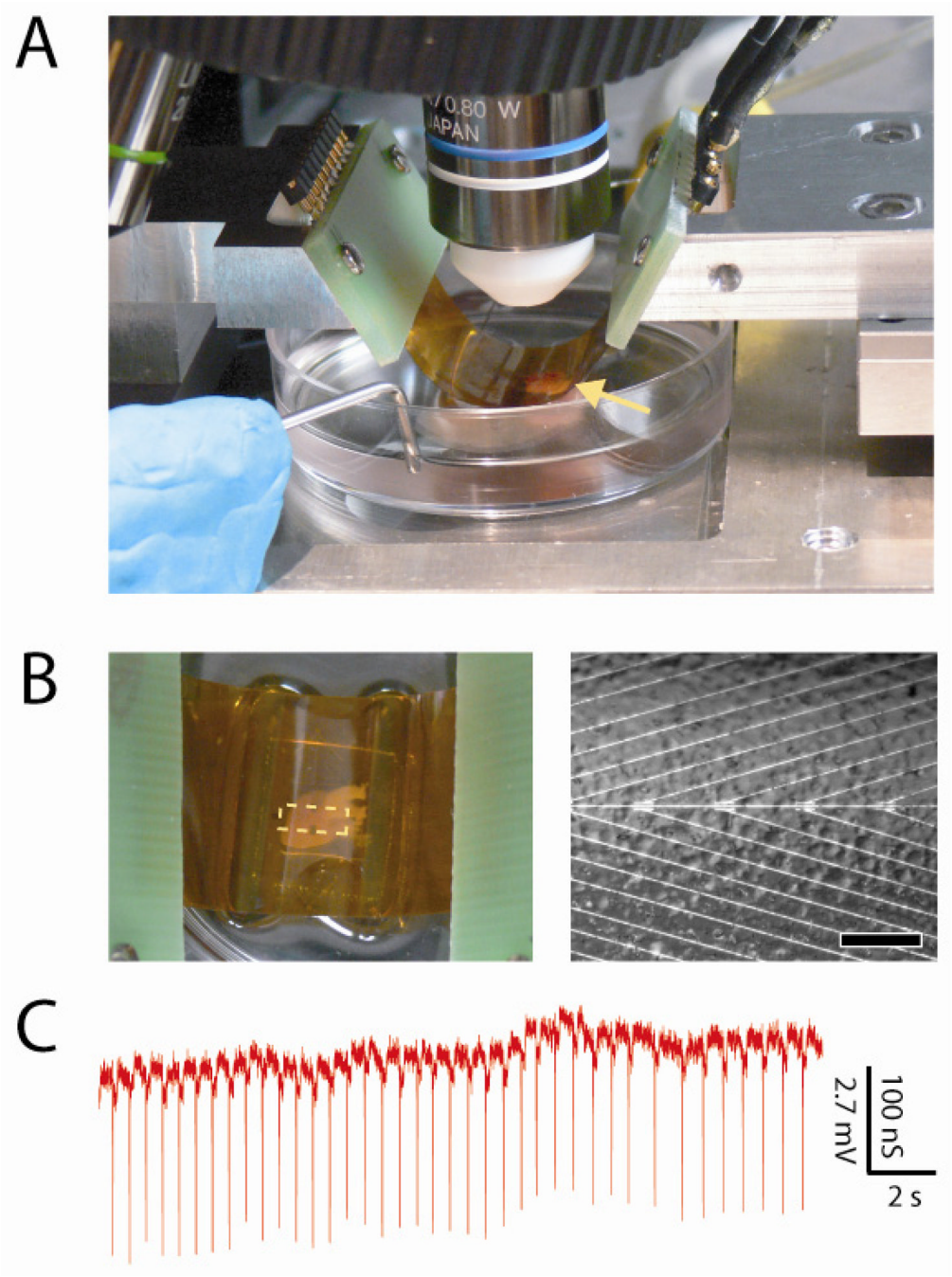

Figure 3. NWFET recording in bent chip configurations

(A) Photograph of heart (yellow arrow) located underneath bent substrate with devices on lower concave face of the substrate. (B) (left) Top-down photograph of same system, enabling overall registration between heart and lithographically-defined markers on the substrate. The dashed white rectangle at the center of the chip highlights the location of NWFET array. (right) Optical microscopy image taken with same system showing features on the heart surface versus position of individual NW devices, which are located along the central horizontal axis. Scale bar is 150 μm. (C) Recorded conductance data from an NWFET device in the configuration shown in panel A; the voltage calibration was determined from water-gate data recorded on the same device.